Journal of Thermoplastic Composite Materials
http://jtc.sagepub.com

Analysis of Process-Induced Residual Stresses in Tape Placement

Fazil O. Sonmez, H. Thomas Hahn and Mustafa Akbulut

Journal of Thermoplastic Composite Materials 2002; 15; 525
DOI: 10.1177/0892705702015006207

The online version of this article can be found at:
http://jtc.sagepub.com/cgi/content/abstract/15/6/525

Published by:
SAGE Publications
http://www.sagepublications.com

Analysis of Process-Induced Residual Stresses in Tape Placement

FAZIL O. SONMEZ,[1,*] H. THOMAS HAHN[2] AND MUSTAFA AKBULUT[1]

[1]*Department of Mechanical Engineering, Bogazici University Istanbul, Bebek 80815 Turkiye*

[2]*Mechanical and Aerospace Engineering Department UCLA, Los Angeles CA 90024, USA*

ABSTRACT: The tape placement for thermoplastic composites involves heating, melting, and cooling steps just as do the other manufacturing processes. Consequently, development of residual stresses is unavoidable due to disparate thermal characteristics of matrix and fiber materials and also due to nonuniform cooling rates. From the product quality standpoint, such as interlaminar strength, dimensional accuracy etc., these stresses should be kept within allowable limits.

In this study, a thermoviscoelastic finite element model was developed to predict residual stresses induced during the placement of thermoplastic composite tapes. The process, being continuous, was considered to be under a quasi steady state where process conditions do not change with respect to the moving roller. Relaxation of the residual stresses in previously laid layers was also allowed for.

Results were obtained for both unidirectional and cross-ply laminates. They show the residual stress distributions through the thickness for a number of chosen sets of process parameters (e.g., roller velocity and heat input). Therefore, residual stresses in a laminate can be controlled by modifying these process parameters.

KEY WORDS: thermoplastic composite laminates, APC-2, residual stresses, finite element analysis (FEA).

INTRODUCTION

PROCESSING OF THERMOPLASTIC composites inevitably involves residual stress development. Residual stresses can lead to distortion of finished components, matrix cracking, and inter-ply delaminations [1,2]. Tensile

*Author to whom correspondence should be addressed. E-mail: sonmezfa@boun.edu.tr

0892-7057/02/06 0525–20 $10.00/0 DOI: 10.1106/089270502023207

stresses may even reach to a significant fraction of the tensile strength. Therefore, to ensure reliable and satisfactory performance, residual stresses within a composite part should be known before the part is put into use.

Unacceptably high levels of stress may arise because of two factors. First of all, thermal expansion behavior of fiber-reinforced thermoplastic composites is highly anisotropic. This is due to the large discrepancy in the thermal expansion coefficients of the matrix and fiber materials. In a typical carbon-reinforced unidirectional thermoplastic composite, a temperature increase induces considerable expansion of the laminate in the transverse direction but almost none along the fiber direction. Besides, fibers, being themselves anisotropic, contribute to this effect. The other factor is the temperature gradients induced during the cooling process. This is because of the fact that, when different regions of the composite experience different temperature histories and stiffness properties of the material vary with the temperature, deformation behavior will be incompatible. Although elastic properties of fibers are almost unaffected by temperature, influence of temperature on the properties of the polymer matrix is drastic. Also high processing temperatures typical for high performance thermoplastic composites exacerbate both the effect of temperature gradients and the effect of anisotropic thermal expansion behavior.

The tape placement process is one of the few techniques that have the potential to continuously process thermoplastic composites in large scale industrial production. In the process, an incoming composite tape is bonded to the previously laid and consolidated laminate under heat and pressure locally applied to the interface (Figure 1). By laying additional layers in different directions, a part with desired thickness and properties can be fabricated. Since heat is mainly supplied to the region where the tape and the laminate meet, the process is highly nonisothermal and, residual stresses may become critical. The process poses a very challenging problem of determining residual stresses for the following reason: The tape placement is a continuous process. As such, when a new layer is being placed, the previously laid and consolidated layers are again subjected to heating. If the temperature of these layers exceeds the glass transition temperature, annealing will ensue and the residual stresses developed during previous tape placement will relax.

Most of the previous studies on the prediction of residual stresses developed during thermoplastic composite processing concentrated on press molding [2–12]. On the other hand, Nejhad et al. [13] proposed a model to predict process induced stresses in filament winding. They modeled filament winding as a transient process. Since this led to excessive computational time, residual stresses could not be obtained within a reasonable time. As for

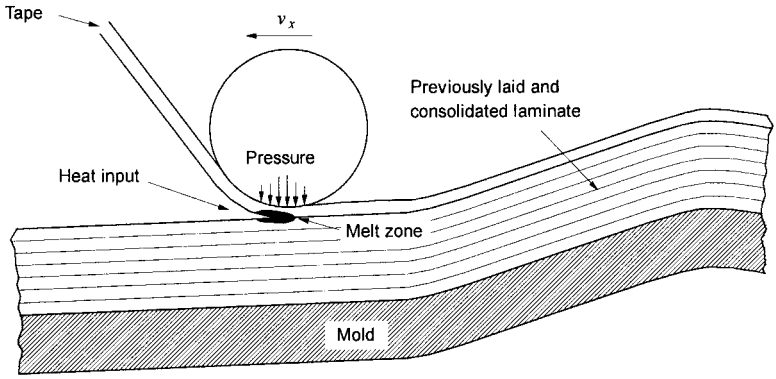

Figure 1. *The thermoplastic composite tape placement process.*

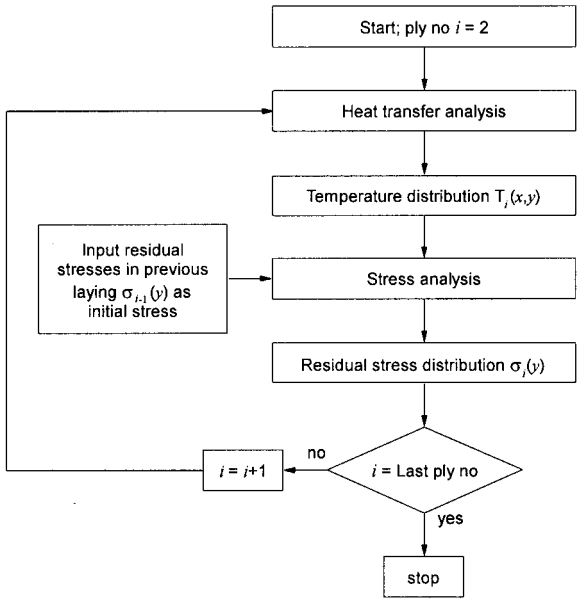

Figure 2. *The solution procedure.*

the modeling of residual stresses in tape placement, the present study is, as far as the authors know, the first of its kind.

Figure 2 shows the solution procedure used in the analysis. The thermal and stress analyses are coupled. The temperature field generated by the thermal analysis is used in the stress analysis to calculate thermal strains and

shift factors. Since a different kind of mesh structure is utilized in the stress analysis, the temperature field determined by the thermal analysis is mapped onto the grid used in the stress analysis by a linear interpolation. In order to account for the relaxation of residual stresses in previously laid layers, residual stresses calculated during the placement of the last ply are used as initial stresses for the current configuration.

HEAT TRANSFER ANALYSIS

The previously developed model for heat transfer in the tape placement process [14] was used, but generalized to account for cross-ply lay-ups.

STRESS ANALYSIS

The residual stress model used in the present study is also an extension of the model that was developed to predict instantaneous stress distribution under the roller [15]. The model was generalized to account for cross-ply lay-ups. Because the objective in this study was to determine residual stresses after the completion of tape placement process rather than the instantaneous stress field under the roller, the mesh structure was changed. Instead of a mesh whose elements are concentrated under the roller, a mesh having lengthwise uniform elements is used. A vertical shift factor was introduced for the creep compliance. Temperature increase not only accelerates the relaxation process but also increases long term compliance (S_∞), which has considerable effect on the residual stress level. Besides, the original finite element formulation was modified to account for the residual stresses developed during the placement of the previous layers.

Formulation of the Problem

ASSUMPTIONS

Fabrication of 3D structures having smooth surfaces is possible in the tape placement process. Tapes can be placed even on nongeodesic paths. But, in this study a basic geometry was chosen to simplify the analysis and interpretation of its results. Specifically, the laminate was assumed to be flat with a unidirectional or a cross-ply lay-up. Although, in practice, the roller should be narrow to accommodate curved contours, it was assumed to be as wide as the laminate itself in the present study, so that a state of plane strain could be used (Figure 3). The effect of crystallization on residual stress development was assumed to be negligible as some previous studies [6,12] had found it to be. The roller was assumed to move with a constant

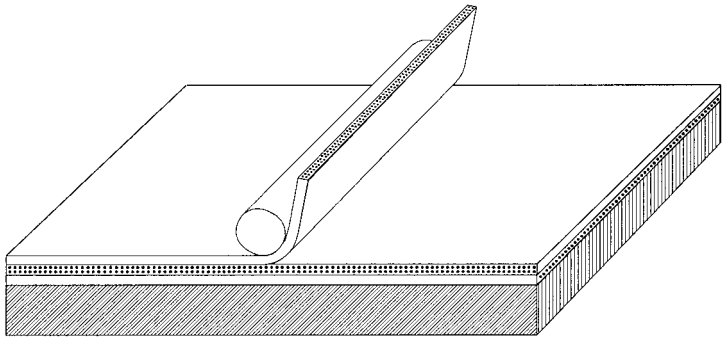

Figure 3. *Analyzed configuration of the process.*

velocity v_x. A steady state was thus assumed to exist within the Eulerian control volume moving with the roller away from an edge.

CONSTITUTIVE RELATIONS

In the analysis, linear constitutive relations were used. Displacement gradients $u_{i,j}$ are much smaller than unity. In several studies [3,6], curvature of unbalanced APC-2 laminates was used as a measure of residual stresses during thermal processing. From these studies, it may be concluded that a significant portion of the residual stresses builds up between just above the glass transition temperature (T_g) and the room temperature. Time dependent response of the material was reported to be dominated by the viscoelastic process close to T_g [16]. Nonlinear and viscoplastic effects can therefore be neglected without compromising the accuracy of the results.

For a continuous unidirectional fiber-reinforced composite having a viscoelastic matrix, the creep compliances S_{11} and S_{12} can be taken to be independent of time and temperature [16,17], where "1" denotes the fiber direction and "2" denotes the transverse direction. The plane of the transverse isotropy is 2–3 plane, and the roller moves in the x direction. The constitutive relations appropriate for this case are expressed as [18–20]

$$\begin{aligned}
\varepsilon_x(t) - \varepsilon_x^*(t) &= S_{11}\sigma_x(t) + S_{12}\sigma_y(t) + S_{12}\sigma_z(t) \\
\varepsilon_y(t) - \varepsilon_y^*(t) &= S_{12}\sigma_x(t) + \int_0^t V_{22}(\tau)S_{22}(\xi - \xi')\frac{\partial \sigma_y(\tau)}{\partial \tau}\,d\tau \\
&\quad + \int_0^t V_{23}(\tau)S_{23}(\xi - \xi')\frac{\partial \sigma_z(\tau)}{\partial \tau}\,d\tau \\
2\varepsilon_{xy}(t) &= \int_0^t V_{66}(\tau)S_{66}(\xi - \xi')\frac{\partial \sigma_{xy}(\tau)}{\partial \tau}\,d\tau
\end{aligned} \tag{1}$$

where $\varepsilon_x^*(t)$ and $\varepsilon_y^*(t)$ are the thermal strains. Note that a state of plane strain with $\varepsilon_z = 0$ is assumed. Since the thermal expansion coefficients, α_i, are temperature dependent, they are given by

$$\varepsilon_i^*(t) = \int_{T_o}^{T_f} \alpha_i(T)\, dT \tag{2}$$

The symbols ξ and ξ' are the pseudo times, which represent the dependence of the creep compliance on temperature. They are given by

$$\xi = \int_0^t a[T(\eta)]\, d\eta \quad \text{and} \quad \xi' = \int_0^\tau a[T(\eta)]\, d\eta \tag{3}$$

$a(T)$ is the horizontal shift factor required to shift the modulus–time curve at temperature T to the one at the base temperature T_{base}. When T is less than T_{base}, $a(T)$ is smaller than 1, and vice versa. This means that accelerated viscoelastic processes within the material at a higher temperature are reflected in a faster elapse of time. $V(T)$ is the vertical shift factor introduced to account for the increase in long term creep compliance $S(\infty)$ with the increasing in temperature.

When the roller moves normal to the fibers, the resulting constitutive relations are

$$\begin{aligned}
\varepsilon_x(t) - \varepsilon_x^*(t) &= \int_0^t V_{22}(T) S_{22}(\xi - \xi') \frac{\partial \sigma_x(\tau)}{\partial \tau} d\tau \\
&\quad + \int_0^t V_{23}(T) S_{23}(\xi - \xi') \frac{\partial \sigma_y(\tau)}{\partial \tau} d\tau + S_{12}\sigma_z(t) \\
\varepsilon_y(t) - \varepsilon_y^*(t) &= \int_0^t V_{23}(T) S_{23}(\xi - \xi') \frac{\partial \sigma_x(\tau)}{\partial \tau} d\tau \\
&\quad + \int_0^t V_{22}(T) S_{22}(\xi - \xi') \frac{\partial \sigma_y(\tau)}{\partial \tau} d\tau + S_{12}\sigma_z(t) \\
2\varepsilon_{xy}(t) &= \int_0^t [S_{22}(\xi - \xi') - S_{23}(\xi - \xi')] \frac{d\sigma_{xy}(\tau)}{d\tau} d\tau
\end{aligned} \tag{4}$$

BOUNDARY CONDITIONS

The laminate rests on a rigid mold. Therefore, at the bottom surface, the following boundary condition is met:

$$u_y = 0 \tag{5}$$

At the left side of the control volume, the initial stress (σ_x) is equal to the residual stress developed during the placement of the previous ply:

$$\sigma_x(x, y)\big|_{x=0} = \sigma_{i-1}(y) \tag{6}$$

The control volume is sufficiently large so that the stress gradients are zero at the right and left sides:

$$\frac{\partial \sigma}{\partial x} = 0 \tag{7}$$

This condition can be achieved, only if the temperature gradients are also equal to zero. This means the control volume should be taken so large that the temperature at the right edge is the same as the ambient temperature. With the condition of constant temperature, stresses also remain constant. Therefore, the stress state at the right edge of the control volume represents residual stresses.

Because we assume linear constitutive relations, namely a relation which is independent of the level of stress, the force applied by the roller on the laminate is not included in the analysis. The roller induces instantaneous stresses which quickly decay to zero as soon as the roller passes. Therefore, we assume that the roller force has no effect on the development of residual stresses.

Finite Element Solution of the Problem

Since the roller moves with a constant velocity, we use the assumption of a quasi-steady state neglecting the inertia effect. Of course, such assumption does not hold true near the edges of the part. Thus, the results of the present analysis are valid away from the edges.

The quasi-steady state assumption permits the use of a control volume which moves with the roller. The control volume is taken as stationary and the material body moves through the control volume. The control volume to be analyzed is divided into eight-degrees-of-freedom rectangular elements as shown in Figure 4. The material body thus moves through the control volume to the right.

The strain in a finite element is a linear function of the eight nodal displacements [21]:

$$\{\varepsilon\}_r = [A]_r\{\delta\}_r \tag{8}$$

where $[A]_r$ is a 3×8 matrix whose elements depend only on the nodal displacements of the element r, $\{\delta\}_r$.

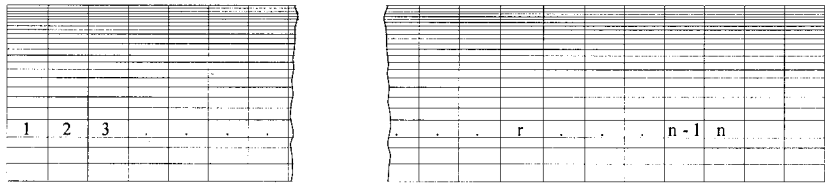

Figure 4. *Mesh structure used in the stress analysis. Horizontal and vertical dimensions are not to scale.*

Consider the material element which occupies the control volume element n at time t_n. We note that this material element was at the control volume element 1 at time t_1, at the control volume element 2 at time t_2, etc., Figure 4. The viscoelastic memory dependence of this material element implies that the stress state in the control volume element n at t_n be determined by the strains in all elements $1, 2, \ldots, (n-1)$ which the material element passed through previously [22,23]. Thus, the stress components in the finite element n can be found by converting the convolution integrals in Equation (1) into a summation of series and reducing the relation to the following form (Appendix A):

$$\begin{Bmatrix} \sigma_x^n \\ \sigma_y^n \\ \sigma_{xy}^n \end{Bmatrix} = \sum_{r=1}^{n} \begin{bmatrix} c_{11}^{nr} & c_{12}^{nr} & 0 \\ c_{12}^{nr} & c_{22}^{nr} & 0 \\ 0 & 0 & c_{66}^{nr} \end{bmatrix} \begin{Bmatrix} \varepsilon_x^r - \varepsilon_x^{*r} + \varepsilon_x^0 \\ \varepsilon_y^r - \varepsilon_y^{*r} + \varepsilon_y^0 \\ 2\varepsilon_{xy}^r \end{Bmatrix} \tag{9}$$

or

$$\{\sigma\}_n = \sum_{r=1}^{n} [C]_{nr}\{\varepsilon\}_r - \sum_{r=1}^{n} [C]_{nr}\{\varepsilon^*\}_r + \sum_{r=1}^{n} [C]_{nr}\{\varepsilon_0\} \tag{10}$$

where $\{\varepsilon^*\}_r$ is the thermal strain vector [15] whose elements depend only on the nodal temperatures of the element r, and $\{\varepsilon_o\}$ is the initial strain vector representing residual stresses developed during the placement of previous layers.

Combining Equations (8) and (10), we obtain

$$\{\sigma\}_n = \sum_{r=1}^{n} [C]_{nr}[A]_r\{\delta\}_r - \sum_{r=1}^{n} [C]_{nr}\{\varepsilon^*\}_r + \sum_{r=1}^{n} [C]_{nr}\{\varepsilon_0\} \tag{11}$$

The virtual work principle requires that

$$\{\delta\}_n^T\{F\}_n = \int_{V_n} \{\varepsilon\}_n^T\{\sigma\}_n dV_n \tag{12}$$

where $\{F\}_n$ is the vector of forces acting at the nodal points of the element n, and V_n is its volume. Substituting Equations (8) and (11) into Equation (12) yields

$$\{\delta\}_n^T\{F\}_n = \int_{V_n} \{\delta\}_n^T[A]_n^T\left[\sum_{r=1}^{n}[C]_{nr}[A]_r\{\delta\}_r - \sum_{r=1}^{n}[C]_{nr}\{\varepsilon^*\}_r + \sum_{r=1}^{n}[C]_{nr}\{\varepsilon_0\}\right]dV_n \tag{13}$$

Therefore,

$$\{F\}_n = \int_{V_n}\sum_{r=1}^{n}[A]_n^T[C]_{nr}[A]_r\{\delta\}_r\,dV_n - \int_{V_n}\sum_{r=1}^{n}[A]_n^T[C]_{nr}\{\varepsilon^*\}_r\,dV_n + \int_{V_n}\sum_{r=1}^{n}[A]_n^T[C]_{nr}\{\varepsilon_0\}\,dV_n \tag{14}$$

or,

$$\{F\}_n = \sum_{r=1}^{n}[K]_{nr}\{\delta\}_r + \sum_{r=1}^{n}\{H\}_{nr} + \sum_{r=1}^{n}\{H_0\} \tag{15}$$

Here $[K]_{nr}$ is the effective element stiffness matrix, $\{H\}_{nr}$ is the effective thermal force vector, and $\{H_0\}$ is the effective initial force vector.

Components of the element stiffness matrix and the thermal force vector are given in [24]. By following the procedure in [15], the global stiffness equation for the entire control volume can be obtained from the element stiffness equations (Equation (15)), and solved to determine the stress field within the control volume. The stress state of the material exiting the control volume can then be taken to be the same as the residual stress developed after the placement of the layer.

RESULTS AND DISCUSSIONS

A computer code was developed following the aforementioned solution procedure and the effects of the processing parameters such as roller speed on the residual stress distribution within the laminate were investigated. The processed material was chosen to be APC-2.

Inputs for the FEM Code

Most of the inputs for the heat transfer and stress analysis were given in [14,15]. Xiao [16] provided the data regarding the creep compliances and the

Table 1. Vertical shift factors for APC-2.

Temperature (°C)	Vertical Shift Factor (log V)
40	−0.025
129.4	+0.0031
200	+0.21

shift factors. Vertical shift factors reported by Xiao [16] were extrapolated, as was done in [7,25] (Table 1).

Barnes et al. [26,27] characterized the anisotropic thermal expansion behavior of APC-2. Jeronimidis and Parkyn [3] determined the stress free temperature by heating up unbalanced laminates and observing the temperature at which they became flat. They found it to be 310°C. Another study [6] found the stress free temperature to be 280°C. However, the residual stress model was observed to be not very sensitive to the value of stress free temperature. The results did not show appreciable differences between the two values of stress free temperature. In the present study, therefore, the base temperature, T_{base}, was taken to be 280°C and the effect of thermal expansion on residual stress development was neglected above this temperature by taking thermal expansion coefficients as zero.

In order to ensure convergence, the length of the control volume was chosen to be 4 m, and the finite element mesh to be 120×24.

Verification

Due to the lack of experimental data on the tape placement process, our model was verified using the results of the press molding process. The numerical results were compared with experimental data for two cases. One is a unidirectional laminate, $[0_{40}]$, processed at 35°C/s surface cooling rate, and the other a cross-ply laminate, $[0_{10}/90_{10}]_s$ processes at 0.25°C/s surface cooling rate. As seen in Figures 5 and 6, the residual stress model agrees quite well with the experimental data. Because the modified version of the residual stress model for press molding was verified, we assumed that predictions of the residual stress model developed for tape placement were reliable.

The Effect of Process Variables

The thermomechanical history determines the resulting residual stress in a viscoelastic material. Therefore, in the present study we chose the process variables that influence temperature distribution and examined their effects

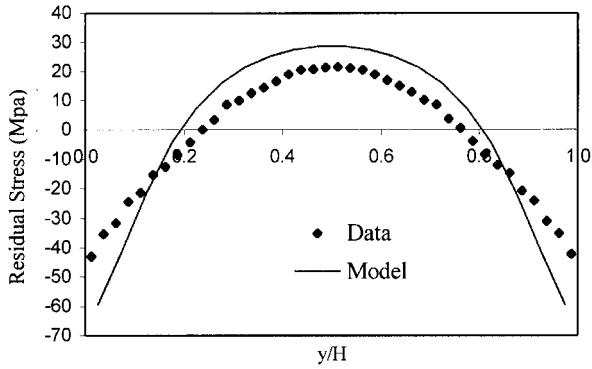

Figure 5. *Transverse normal residual stress distribution within a 40 ply APC-2 unidirectional laminate, $[0_{40}]_T$, processed by press molding at a 35°C/s surface cooling rate. Experimental data were obtained by a layer removal technique [28].*

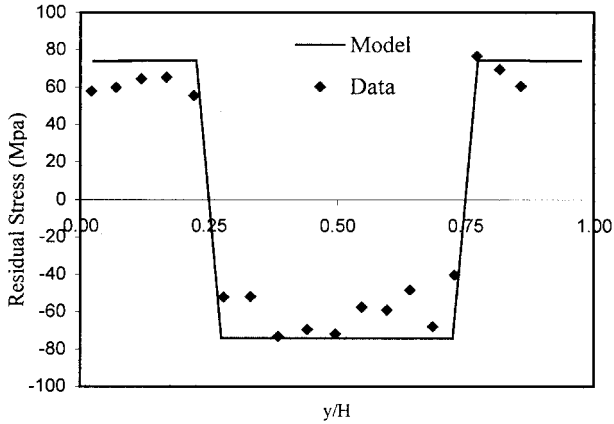

Figure 6. *Normal stress distribution within a cross-ply laminate, $[0_{10}/90_{10}]_s$, processed by press molding at a 0.25°C/s surface cooling rate. Experimental data were obtained by a layer removal technique [11].*

on residual stress. Figure 7 shows the process variables under consideration. The default values are 16 mm/s for roller velocity (v_x), 1.0 for the ratio of heated substrate length to heated tape length ($\eta = hls/hl$). The hot gas temperature is taken as 600°C. The results show the maximum tensile residual stress at the end of 16-ply lay-up, $[0_4/90_4]_s$.

Preheating the laminate to a certain temperature before placing the tape is a usual practice to help bonding. If the preheating temperature is increased, the temperature difference between the heated zone and the remaining region

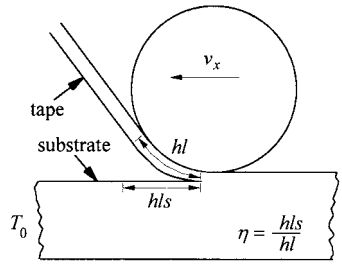

Figure 7. *Process variables of tape placement.*

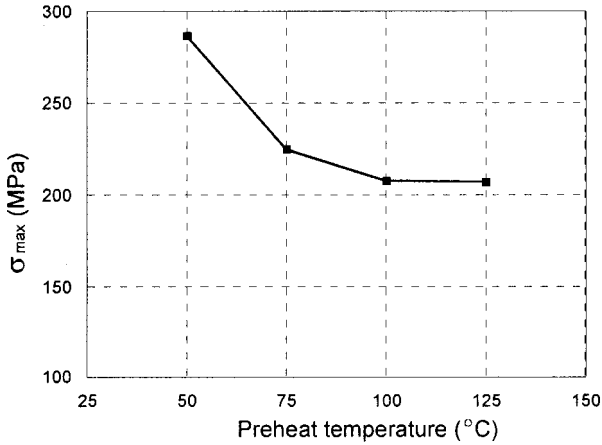

Figure 8. *The effect of preheat temperature on the maximum tensile stress, σ_x.*

becomes smaller, and the material cools more slowly [14]. Consequently residual stresses decrease as Figure 8 indicates.

Figure 9 shows increasing roller velocity leading to a higher level of residual stress. This is because, at high speeds, only regions close to the heated surface are raised to high temperatures [14]. Localized heating causes higher temperature gradients, and thus higher residual stresses.

As our previous study [14] showed, the lengths of the heated surfaces on the tape and substrate significantly affect the temperature distribution. The effect of larger heated lengths is similar to the effect of preheating the substrate in slowing down the cooling rate. In contrast, a small heated length results in a highly localized heated zone and thus higher residual stresses as suggested by Figure 10.

In the above results, both the tape and the substrate were heated equally. Supplying more heat to the substrate by increasing the surface exposed to hot gas was found to result in a more uniform temperature distribution [14].

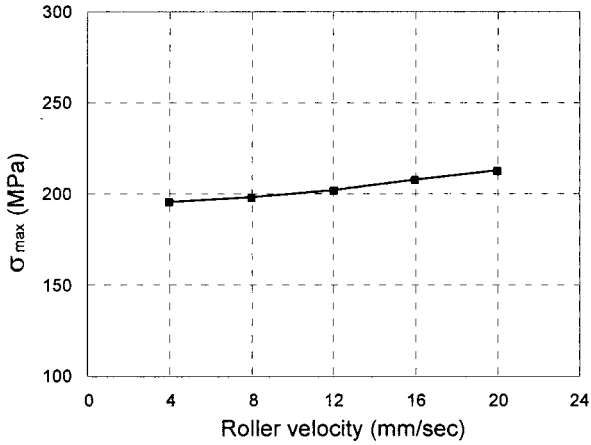

Figure 9. *The effect of roller velocity on the maximum tensile stress, σ_x.*

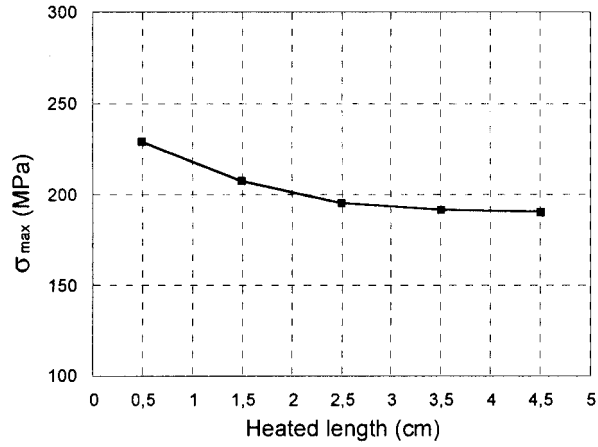

Figure 10. *The effect of heated length on the maximum tensile stresses.*

Figure 11 indeed shows that increasing the ratio of heated substrate length to heated tape length reduces the maximum tensile residual stress. In these runs, the heated length on tape was kept constant at 1.5 cm while the heated length on substrate was increased from 1.5 to 4.5 cm, then to 7.5 cm, and finally to 10.5 cm.

Figure 12 shows residual stress (σ_{xx}) distribution through the thickness of a cross-ply laminate, $[0_4/90_4]_s$. Ply numbers 1 and 16 indicate the top and bottom layers, respectively. The distribution is uneven through the thickness of the laminate. Compressive stresses develop in the top and bottom 4 plies

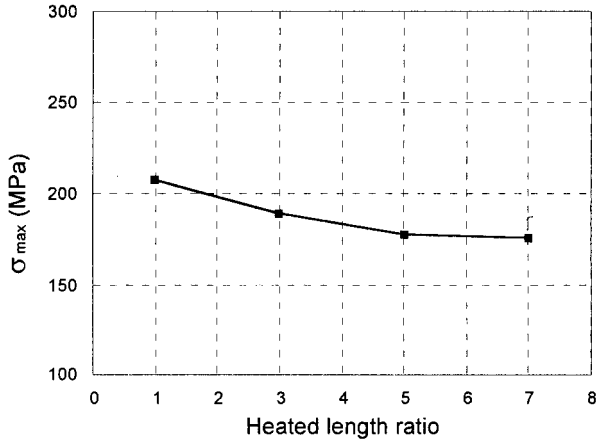

Figure 11. *The effect of heated length ratio on the maximum tensile stress.*

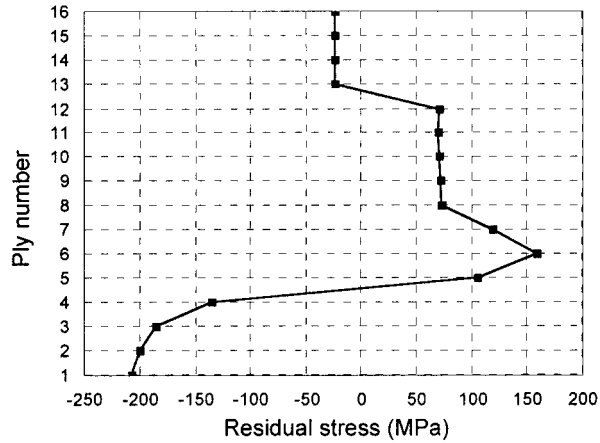

Figure 12. *Residual stress (σ_{xx}) distribution through the thickness of a 16 ply cross-ply laminate.*

while tensile stresses develop in the middle 8 plies. These stresses are high enough to cause undesirable distortions in the laminate. The tensile stresses occurring in the middle plies are high enough to cause matrix cracking.

CONCLUSIONS

A residual stress analysis was carried out for the tape placement process, and the effects of process parameters on residual stress distributions were

investigated through a parametric study. The process parameters that affect the temperature distribution were found to affect the residual stresses. Any changes in process parameters leading to a more localized temperature distribution lead to higher residual stresses. The chosen sets of process parameters resulted in quite high residual stresses, much higher than the levels encountered in press molding.

Residual stresses accumulate gradually during successive lay-down of layers, they may reach excessively high levels especially in thick laminates. Furthermore, unsymmetrical distribution of residual stresses can lead to the distortion of finished products. Thus, process parameters should be optimized to minimize residual stresses and, at the same time, reduce the uneven distribution. This can be achieved by combining the present process model with an optimization algorithm. Otherwise, post-processing may be needed.

In the present investigation we only examined the effects of process parameters on residual stresses. We have not considered other criteria for product quality such as consolidation, crystallinity or degradation. A full optimization of process parameters should include these other quality criteria as well.

ACKNOWLEDGMENT

This paper is based on the work supported by the Research Fund of Bogazici University with the code number 97HA602.

APPENDIX A

Numerical Integration of the Constitutive Equations

Rewriting constitutive equation for shear strain given in Equation (1), we have

$$2\varepsilon_{xy}(t) = \int_0^t V_{66}(T(\tau))S_{66}(\xi(t) - \xi'(\tau))\frac{\partial\sigma_{xy}(\tau)}{\partial\tau}d\tau \tag{A.1}$$

where *pseudo-time*, ξ, is related to the real time by

$$\xi = \int_0^t a[T(x_i, \eta)\, d\eta \tag{A.2}$$

where $a(T)$ is the *horizontal shift factor*. The above integral can easily be calculated numerically.

Applying integration by parts to Equation (A.1), one obtains

$$2\varepsilon_{xy}(t) = \sigma_{xy}(\tau)\, V_{66}(T(\tau))S_{66}(\xi(t)-\xi'(\tau))\Big|_0^t - \int_0^t \sigma_{xy}(\tau)\frac{\partial[V_{66}(T(\tau))S_{66}(\xi(t)-\xi'(\tau))]}{\partial\tau}d\tau \tag{A.3}$$

then,

$$2\varepsilon_{xy}(t) = \sigma_{xy}(t)V_{66}(V(t))S_{66}(0) - \sigma_{xy}(0)V(T(0))S_{66}(\xi(t)) - \int_0^t \sigma_{xy}(\tau)\frac{\partial[V_{66}(T(\tau))S_{66}(\xi(t)-\xi'(\tau))]}{\partial\tau}d\tau \tag{A.4}$$

where the second term represents the initial stress.

Equation (A.4) can be integrated using finite differences in time. Consider incremental times t_i or $\xi_i(t_i)$ $(i=1,2,\ldots,r,\ldots,n)$, where t_r is the time at which the material is in the control volume element r (Figure 4), ($t_1=0$ and $t_n=t$). Utilizing the second mean value theorem, we can express the strain in the control volume element n as

$$\begin{aligned}2\varepsilon_{xy}(t_n) = {} & \sigma_{xy}(t_n)V_{66}(T_n)S_{66}(0) - \sigma_{xy}(t_1)V_{66}(T_1)S_{66}(\xi(t_n)) \\ & -\frac{1}{2}\sum_{r=1}^{n-1}\left[\sigma_{xy}(t_{r+1})+\sigma_{xy}(t_r)\right] \\ & \times\left[V_{66}(T_{r+1})S_{66}(\xi_n-\xi_{r+1}) - V_{66}(T_r)S_{66}(\xi_n-\xi_r)\right]\end{aligned} \tag{A.5}$$

Thus Equation (1) can be reduced to the following form:

$$\begin{Bmatrix}\varepsilon_x(t_n)\\ \varepsilon_y(t_n)\\ 2\varepsilon_{xy}(t_n)\end{Bmatrix} = \sum_{r=1}^{n}\begin{bmatrix}d_{11}^{nr} & d_{12}^{nr} & 0\\ d_{12}^{nr} & d_{22}^{nr} & 0\\ 0 & 0 & d_{66}^{nr}\end{bmatrix}\begin{Bmatrix}\sigma_x(t_r)\\ \sigma_y(t_r)\\ \sigma_{xy}(t_r)\end{Bmatrix} + \begin{Bmatrix}\varepsilon_x^*(t_n)\\ \varepsilon_y^*(t_n)\\ 0\end{Bmatrix} - \begin{Bmatrix}\varepsilon_x^0\\ \varepsilon_y^0\\ 2\varepsilon_{xy}^0\end{Bmatrix} \tag{A.6}$$

or

$$\{\varepsilon\}_n = \sum_{r=1}^{n}[D]_{nr}\{\sigma\}_r + \{\varepsilon^*\}_n - \{\varepsilon_0\}$$

where

$$d_{11}^{nr} = \begin{cases}0 & r\neq n\\ S_{11} & r=n\end{cases} \tag{A.7}$$

$$d_{12}^{nr} = \begin{cases} 0 & r \neq n \\ S_{12} & r = n \end{cases} \tag{A.8}$$

$$d_{22}^{nr} = \begin{cases} -\frac{1}{2}\{V_{22}(T_1)S_{22}(\xi_n) + V_{22}(T_2)S_{22}(\xi_n - \xi_2)\} & r = 1,\ n \neq 1 \\ \frac{1}{2}\{V_{22}(T_{r-1})S_{22}(\xi_n - \xi_{r-1}) - V_{22}(T_{r+1})S_{22}(\xi_n - \xi_{r+1})\} & 1 < r < n \\ V_{22}(T_1)S_{22}(\xi_1) & r = n = 1 \\ \frac{1}{2}\{V_{22}(T_{n-1})S_{22}(\xi_1) + V_{22}(T_n)S_{22}(\xi_n - \xi_{n-1})\} & r = n \neq 1 \end{cases} \tag{A.9}$$

$$d_{66}^{nr} = \begin{cases} -\frac{1}{2}\{V_{66}(T_1)S_{66}(\xi_n) + V_{66}(T_2)S_{66}(\xi_n - \xi_2)\} & r = 1,\ n \neq 1 \\ \frac{1}{2}\{V_{66}(T_{r-1})S_{66}(\xi_n - \xi_{r-1}) - V_{66}(T_{r+1})S_{66}(\xi_n - \xi_{r+1})\} & 1 < r < n \\ V_{66}(T_1)S_{66}(\xi_1) & r = n = 1 \\ \frac{1}{2}\{V_{66}(T_{n-1})S_{66}(\xi_1) + V_{66}(T_n)S_{66}(\xi_n - \xi_{n-1})\} & r = n \neq 1 \end{cases} \tag{A.10}$$

Here, 1 is the fiber direction, and 2 and 3 are the transverse directions. Initial strains are related to initial stresses by

$$\begin{Bmatrix} \varepsilon_x^0 \\ \varepsilon_y^0 \\ 2\varepsilon_{xy}^0 \end{Bmatrix} = \begin{bmatrix} S_{11}(0) & S_{12}(0) & 0 \\ S_{12}(0) & V_{22}(T_1)S_{22}(\xi(t_n)) & 0 \\ 0 & 0 & V_{66}(T_1)S_{66}(\xi(t_n)) \end{bmatrix} \begin{Bmatrix} \sigma_x^0 \\ \sigma_y^0 \\ 2\sigma_{xy}^0 \end{Bmatrix} \tag{A.11}$$

Strain–stress relations given by Equations (A.6) and (A.11) in numerical form are valid for plane stress. But in our model, we assumed plane-strain state. For plane strain, when the directions of roller movement, x, and the fiber direction, 1, coincide, (A.6) becomes

$$\begin{Bmatrix} \varepsilon_x(t_n) \\ \varepsilon_y(t_n) \\ 2\varepsilon_{xy}(t_n) \end{Bmatrix} = \sum_{r-1}^{n} \begin{bmatrix} d_{11}^{nr} - (d_{12}^{nr})^2/d_{12}^{nr} & d_{12}^{nr} - d_{12}^{nr}\, d_{23}^{nr}/d_{22}^{nr} & 0 \\ d_{12}^{nr} - d_{12}^{nr}\, d_{23}^{nr}/d_{22}^{nr} & d_{22}^{nr} - (d_{23}^{nr})^2/d_{22}^{nr} & 0 \\ 0 & 0 & d_{66}^{nr} \end{bmatrix} \begin{Bmatrix} \sigma_x(t_r) \\ \sigma_y(t_r) \\ \sigma_{xy}(t_r) \end{Bmatrix} + \begin{Bmatrix} \varepsilon_x^*(t_n) \\ \varepsilon_y^*(t_n) \\ 0 \end{Bmatrix} - \begin{Bmatrix} \varepsilon_x^0 \\ \varepsilon_y^0 \\ 2\varepsilon_{xy}^0 \end{Bmatrix} \tag{A.12}$$

Assuming that the Poisson's ratio in the isotropic plane, ν_{23}, is independent of time and temperature, $S_{23}(t)$ is given by

$$S_{23}(t) = -\nu_{23} S_{22}(t) \tag{A.13}$$

Also, the following values should be used for thermal expansion coefficients:

$$\begin{aligned} \alpha_{xx} &= \alpha_{11} + \nu_{31}\alpha_{33} \\ \alpha_{yy} &= \alpha_{22} + \nu_{32}\alpha_{33} \end{aligned} \tag{A.14}$$

For transversely isotropic laminates $\alpha_{33} = \alpha_{22}$, $\nu_{32} = \nu_{23}$ and $\nu_{31} = \nu_{21}$.

When the roller movement is transverse to the fiber direction for a given ply, strain–stress relations for plane strain state become

$$\begin{Bmatrix} \varepsilon_x(t_n) \\ \varepsilon_y(t_n) \\ 2\varepsilon_{xy}(t_n) \end{Bmatrix} = \sum_{r=1}^{n} \begin{bmatrix} d_{22}^{nr} - (d_{12}^{nr})^2/d_{11}^{nr} & -\nu_{23}d_{22}^{nr} - (d_{12}^{nr})^2/d_{11}^{nr} & 0 \\ -\nu_{23}d_{22}^{nr} - (d_{12}^{nr})^2/d_{11}^{nr} & d_{22}^{nr} - (d_{12}^{nr})^2/d_{11}^{nr} & 0 \\ 0 & 0 & 2(1+\nu_{23})d_{22}^{nr} \end{bmatrix}$$

$$\times \begin{Bmatrix} \sigma_x(t_r) \\ \sigma_y(t_r) \\ \sigma_{xy}(t_r) \end{Bmatrix} + \begin{Bmatrix} \varepsilon_x^*(t_n) \\ \varepsilon_y^*(t_n) \\ 0 \end{Bmatrix} - \begin{Bmatrix} \varepsilon_x^0 \\ \varepsilon_y^0 \\ 2\varepsilon_{xy}^0 \end{Bmatrix} \tag{A.15}$$

and thermal expansion coefficients are

$$\alpha_{xx} = \alpha_{yy} = \alpha_{22} + \nu_{12}\alpha_{11} \tag{A.16}$$

Equation (A.12) or (A.15) can be converted to Equation (9), where stress is a dependent variable, by following the procedure described in [15].

REFERENCES

1. Kwon, Y.W. and Berner, J.M. (1997). Matrix damage of fibrous composites: effects of thermal residual stresses and layer sequences. *Computers & Structures*, **64**(1–4): 375–382.
2. Chapman, T.J., Gillespie, J.W., Pipes, R.B., Manson, J.-A.E. and Seferis, J.C. (1990). Prediction of process-induced stresses in thermoplastic composites. *Journal of Composite Materials*, **24**: 616–643.
3. Jeronimidis, G. and Parkyn, A.T. (1988). Residual stresses in carbon fibre-thermoplastic matrix laminates. *Journal of Composite Materials*, **22**: 401–415.

4. Lawrence, W.E., Manson, J.-A.E., Seferis, J.C., Gillespie, J.W. and Pipes, R.B. (1990). Prediction of residual stress in continuous fiber semicrystalline in thermoplastic composites: a kinetic viscoelastic approach. In: *Proceedings of American Society for Composites 5th Technical Conference*. Holiday Inn, 300 MAC, E. Lansing, MI, June 12–14. pp. 401–414.
5. Wang, T.M., Daniel, I.M. and Gotto, J.T. (1992). Thermoviscoelastic analysis of residual stresses and warpage in composite laminates. *Journal of Composite Materials*, **26**(6): 883–899.
6. Unger, W.J. and Hansen, J.S. (1993). The effect of cooling rate and annealing on residual stress development in graphite fibre reinforced PEEK laminates. *Journal of Composite Materials*, **27**(2): 108–137.
7. Lee, K. and Weistman, Y. (1994). Optimal cool down in nonlinear thermoviscoelasticity with application to graphite/PEEK (APC-2) laminates. *Journal of Applied Mechanics*, **61**: 367–374.
8. Li, M.C., Wu, J.J., Loos, A.C. and Morton, J. (1997). A plane-strain finite element model for process-induced stresses in a graphite/PEEK composite. *Journal of Composite Materials*, **31**(3): 212–243.
9. Wang, C. and Sun, C.T. (1997). Thermoelastic behavior of PEEK thermoplastic composite during cooling from forming temperatures. *Journal of Composite Materials*, **31**(22): 2230–2248.
10. Domb, M.M. and Hansen, J.S. (1998). The effect of cooling rate on free-edge stress development in semi-crystalline thermoplastic laminates. *Journal of Composite Materials*, **32**(4): 361–386.
11. Ersoy, N. and Vardar, O. (2000). Measurement of residual stresses in layered composites by compliance method. *Journal of Composite Materials*, **34**(7): 575–598.
12. Ersoy, N.B. (1998). Prediction and measurement of residual stresses in layered composites. PhD Thesis, Bogazici University, Istanbul.
13. Nejhad, M.N.G., Gillespie, J.W. and Cope, Jr. R.D. (1992). Prediction of process-induced stresses for in-situ thermoplastic filament winding of cylinders. In: *Proceedings of 3rd International Conference, Computer Aided Design in Composite Material Technology*. Delaware: Newark. Vol. 3. pp. 277–295.
14. Sonmez, F.O. and Hahn, H.T. (1997). Process modeling of heat transfer and crystallization for thermoplastic composite tape placement. *Journal of Thermoplastic Composite Materials*, **10**(3): 198–240.
15. Sonmez, F.O. and Hahn, H.T. (July 1997). Thermoviscoelastic analysis of the tape placement process. *Journal of Thermoplastic Composite Materials*, **10**(4): 381–414.
16. Xiao, X.R. (1994). Characterization and modeling of nonlinear viscoelastic response of PEEK resin and PEEK composites. *Composites Engineering*, **4**(7): 681–702.
17. Horoschenkoff, A. (1990). Characterization of the creep compliances J_{22} and J_{66} of orthotropic composites with PEEK and epoxy matrices using the nonlinear viscoelastic response of the neat resins. *Journal of Composite Materials*, **24**: 879–891.
18. Morland, L.W. and Lee, E.H. (1960). Stress analysis for linear viscoelastic materials with temperature variation. *Transactions of the Society of Rheology*, **4**: 233–263.
19. Shapery, R.A. (1967). Stress analysis of viscoelastic composite materials. *Composite Materials*, **1**: 228–267.
20. Christensen, R.M. (1982). *Theory of Viscoelasticity*. New York: Academic Press.
21. Yang, T.Y. (1986). *Finite Element Structural Analysis*. New Jersey: Prentice-Hall.
22. Lynch, F. de S. (1969). A finite element method of viscoelastic stress analysis with application to rolling contact problems. *International Journal for Numerical Methods in Engineering*, **1**: 379–394.
23. Batra, R.C. (1977). Cold sheet rolling, the thermoviscoelastic problem. A numerical, solution. *International Journal for Numerical Methods in Engineering*, **11**: 671–682.

24. Sonmez, F.O. (1995). Modeling of the thermoplastic composite tape placement process. PhD Thesis, UCLA, Los Angeles.
25. Lee, K. and Weistman, Y. (1992). Residual thermal stresses in graphite/PEEK (APC-2) laminates. In: Fujiwara, H., Abe, T. and Tanaka, K. (eds.), *Residual Stresses-III*. London: Elsevier Science Publishers Ltd. pp. 31–37.
26. Barnes, J.A., Simms, I.J., Farrow, G.J., Jackson, D., Wostenholm, G. and Yates, B. (1990). Thermal expansion behavior of thermoplastic composite materials. *Journal of Thermoplastic Composite Materials*, **3**: 66–80.
27. Barnes, J.A. (1993). Thermal expansion behavior of thermoplastic composites. *Journal of Material Science*, **28**: 4974–4982.
28. Manson, J.-A. and Seferis, J.C. Internal stress determination by process simulated laminates. In: *SPE ANTEC 1987 Conference Proceedings*. Los Angeles, CA.